Available online at www.sciencedirect.com
ScienceDirect
Journal of Magnetic Resonance 183 (2006) 242–251
JMR Journal of Magnetic Resonance
www.elsevier.com/locate/jmr

Sensitivity enhanced recoupling experiments in solid-state NMR by γ preparation

Navin Khaneja

Division of Engineering and Applied Sciences, Harvard University, Cambridge, MA 02138, USA

Received 22 May 2006; revised 25 August 2006
Available online 25 September 2006

Abstract

In this paper, we introduce a class of dipolar recoupling experiments under magic angle spinning (MAS), which use gamma dependent antiphase polarization during the t_1 evolution period. We show that this helps us to design dipolar recoupling experiments that transfer both components of the transverse magnetization of spin S to a coupled spin I in the mixing step of a 2D NMR experiment. We show that it is possible to design such transfer schemes and make them insensitive to the orientation dependency of the couplings in powders. This helps us to develop sensitivity enhanced 2D NMR experiments of powder samples under MAS.

Keywords: Recoupling; Sensitivity enhanced; MAS

1. Introduction

Nuclear magnetic resonance (NMR) spectroscopy is finding important applications for atomic-resolution structural analysis of biological macromolecules in the solid phase [1–5]. This opens up the possibility of studying insoluble protein structures such as membrane proteins, fibrils, and extracellular matrix proteins which are difficult to analyze using conventional atomic-resolution structure determination methods, including liquid-state NMR and X-ray crystallography. Sensitivity is a critical issue in all these applications. The most advanced solid-state NMR equipment and techniques still require hours and days of signal averaging for a simple two-dimensional (2D) spectroscopy of peptides and proteins in a noncrystalline solid form. This challenge motivates the present paper, where we address a fundamental problem of coherence transfer in solid-state NMR of "powder" samples. We show how to design experiments that are insensitive to orientations of the crystallite in a powder sample and simultaneously transfer both components of transverse magnetization of spin S to a coupled spin I, in the mixing step of the 2D solid state NMR experiment under magic angle spinning. The transfer schemes presented in the paper lead to sensitivity enhanced experiments in solid state NMR, analogous to the sensitivity enhanced experiments widely used in liquid state NMR [6]. Pulse sequences for simultaneous transfer of transverse component of magnetization have recently appeared in solid state NMR literature [7]. Here we present transfer schemes that are independent of the orientations of the crystallite in a powder sample.

In a standard 2D NMR experiment [8], the initial coherence on spin S evolves under the chemical shift ω_s for time t_1 to $S_x \to S_x\cos(\omega_s t_1) + S_y\sin(\omega_s t_1)$. During the mixing step, the x magnetization on spin S is transferred to a coupled spin I, and assuming perfect transfer, $S_x \to I_x$, the spin I precesses under its chemical shift, i.e.,

$$I_x \cos(\omega_s t_1) \to \cos(\omega_s t_1)\{I_x \cos(\omega_I t_2) + I_y \sin(\omega_I t_2)\}.$$

The precession is recorded and the experiment is repeated by incrementing t_1, finally leading to a two dimensional signal in t_1 and t_2 that encodes for ω_I and ω_S. Simultaneous transfer of both components of the transverse magnetization during the mixing step, i.e.,

E-mail address: navin@hrl.harvard.edu

1090-7807/$ - see front matter
doi:10.1016/j.jmr.2006.08.017

$$S_x\cos(\omega_s t_1) + S_y\sin(\omega_s t_1) \rightarrow I_x\cos(\omega_s t_1) + I_y\sin(\omega_s t_1),$$

is desirable as it enhances the sensitivity of the experiment by a factor of $\sqrt{2}$. Such sensitivity enhanced experiments are performed routinely in liquid state NMR [6]. The simultaneous transfer of both transverse components of the magnetization is usually achieved by synthesizing an isotropic Hamiltonian or a Unitary propagator $U_{\text{iso}} = \exp(-i\pi\{I_xS_x + I_yS_y + I_zS_z\})$. However in solid state NMR experiments under MAS, the dispersion in the coupling strengths arising due to the orientation dependence of the couplings makes the task of synthesizing U_{iso} for all coupled spin pairs (independent of the orientation) a non-trivial task. In this paper, we show how this problem can be alleviated by suitably transforming the initial magnetization on spin S, before the t_1 evolution period. We call this step γ *preparation*, as the transformed state depends on angle γ that denotes the rotation of the crystallite around the rotor axis. Specifically, we transform the initial inphase coherence on spin S to an antiphase coherence on spin S, such that the phase of the antiphase coherence on spin S depends on angle γ. This transformed state is then made to evolve under the chemical shift of spin S. Because of the initial preparation, it becomes possible to simultaneously transfer both components of the transverse magnetization of spin S to spin I, after the t_1 precession. This transfer efficiency can be made independent of the angle γ. The basic ideas can be elaborated to devise compensation schemes which also make the transfer efficiency insensitive (to desired level) to angle β expressing the angle between the internuclear axis and the MAS rotor. This results in transfer schemes that approach 100% transfer efficiency for both components of the transverse magnetization.

We note that γ dependent antiphase coherences also arise in context of polarization transfer in many recoupling experiments [21–23]. The main contribution of the paper is to show that it is advantageous to create such antiphase coherences before t_1 evolution as these states allow for simultaneously transfer both components of the transverse magnetization of spin S to spin I after the t_1 precession.

2. Theory

Notation: Let $S_\alpha(\beta,\gamma)$ denote the rotation of operator S_α around the axis β by angle γ, where $\alpha,\beta \in \{x,y,z\}$, i.e., $S_\alpha(\beta,\gamma) = \exp(-i\gamma S_\beta)S_\alpha\exp(i\gamma S_\beta)$. For example $S_x(z,\gamma) = S_x\cos\gamma + S_y\sin\gamma$. It is straightforward to verify that if $[-iS_a, -iS_b] = -iS_c$, then

$$[-iS_a(\beta,\gamma), -iS_b(\beta,\gamma)] = -iS_c(\beta,\gamma).$$

It also follows from definition that for any unitary transformation U,

$$US_\alpha(\beta,\gamma)U' = S_{U\alpha U'}(U\beta U',\gamma),$$

where $S_{U\alpha U'}(U\beta U',\gamma)$, denotes rotation of operator $US_\alpha U'$ around $US_\beta U'$. We will make repeated use of these two properties in the remaining paper.

γ Preparation: Transform the initial coherence on spin S into an antiphase coherence with a phase that depends on γ. More specifically,

$$S_x \rightarrow 2I_z\underbrace{(S_x\cos\gamma - S_y\sin\gamma)}_{S_x(\bar{z},\gamma)}.$$

This can be achieved in a straightforward way by synthesizing an effective Hamiltonian $2I_zS_z(x,\gamma)$ as shown later. During t_1 evolution period, this transformed state evolves under the chemical shift of spin S to a state

$$2I_zS_x(\bar{z},\gamma) \rightarrow 2I_zS_x(\bar{z},\gamma)\cos(\omega_s t_1) + 2I_zS_y(\bar{z},\gamma)\sin(\omega_s t_1),$$

(also written as $2I_zS_x(\bar{z},\gamma-\omega_s t_1)$) and encodes for the chemical shift of spin S. This state can then be transferred by a standard DCP [11] like experiment to $I_x(z,\omega_s t_1) = I_x\cos(\omega_s t_1) + I_y\sin(\omega_s t_1)$ as described below.

Consider two coupled heteronuclear spins I and S under magic angle spinning. The spins are irradiated with rf fields at their Larmor frequencies along say the x-direction. In a double-rotating Zeeman frame, rotating with both the spins at their Larmor frequency, the Hamiltonian of the system takes the form

$$H(t) = \omega_I(t)I_z + \omega_S(t)S_z + \omega_{IS}(t)2I_zS_z + \omega^I_{\text{rf}}(t)I_x + \omega^S_{\text{rf}}(t)S_x, \quad (1)$$

where $\omega_I(t)$, $\omega_S(t)$, and $\omega_{\text{IS}}(t)$ represent time-varying chemical shifts for the two spins I and S and the coupling between them, respectively. These interactions may be expressed as a Fourier series $\omega_\lambda(t) = \sum_{m=-2}^{2}\omega^m_\lambda\exp(im\omega_r t)$, where ω_r is the spinning frequency (in angular units), while the coefficients ω_λ ($\lambda = I,S,IS$) reflect the dependence on the physical parameters like the isotropic chemical shift, anisotropic chemical shift, the dipole–dipole coupling constant and through this the internuclear distance [9]. $\omega^I_{\text{rf}}(t)$ and $\omega^S_{\text{rf}}(t)$ are the amplitudes of the rf fields on spins I and S, respectively. If the rf-field strengths on the two spins is chosen to be integral (or half integral) multiples of the spinning frequency, i.e., $\omega^I_{\text{rf}} = p\omega_r$ and $\omega^S_{\text{rf}} = q\omega_r$, then the Hamiltonian for the dipole–dipole coupling in the interaction frame of the rf-irradiation averages over a rotor period to

$$\begin{aligned}\bar{H} = \frac{1}{4}\{&(\omega_{IS}^{-(p+q)} + \omega_{IS}^{(p+q)})(2I_zS_z - 2I_yS_y) + (\omega_{IS}^{-(p-q)} \\ &+ \omega_{IS}^{(p-q)})(2I_zS_z + 2I_yS_y) - i(\omega_{IS}^{-(p+q)} - \omega_{IS}^{(p+q)})(2I_zS_y \\ &+ 2I_yS_z) + i(\omega_{IS}^{-(p-q)} - \omega_{IS}^{(p-q)})(2I_zS_y - 2I_yS_z)\}. \quad (2)\end{aligned}$$

Choosing $p = 0$ and $q = 1$, we prepare the effective coupling Hamiltonian

$$H_{\text{p}} = \kappa\{2I_zS_z\cos(\gamma) - 2I_zS_y\sin(\gamma)\} = \kappa 2I_zS_z(x,\gamma) \quad (3)$$

where γ as before is the Euler angle discriminating the crystallites by rotations around the rotor axis. The scaling factor $\kappa = \frac{1}{2\sqrt{2}}b_{IS}\sin(2\beta)$ depends on the dipole–dipole coupling constant b_{IS} and the angle β between the internuclear axis and the rotor axis. We, for now, neglect dispersion in κ, and let $H_{\text{p}}(\frac{\pi}{2}) = \frac{\pi}{2}(2I_zS_z(x,\gamma))$ correspond to a $\frac{\pi}{2}$ rotation, obtained by evolving H_{p} for time $\tau = \frac{\pi}{2\kappa_0}$.

Remark 1. In the above analysis we have neglected chemical shift anisotropy (CSA) of spin S. In the presence of CSA, rf irradiation at rotor frequency ω_r will recouple the CSA. An alternate way of synthesizing the effective Hamiltonian $H_p(\frac{\pi}{2})$ (which gets around the problem of CSA recoupling) is to choose $p-q=-1$ and $p,q>2$ (for e.g., $p=3$, $q=4$), for duration τ followed by switching $\omega_{rf}^I = p\omega_r$ to $\omega_{rf}^I = -p\omega_r$ for the remaining τ [10]. The first τ, evolution prepares the effective Hamiltonian $\kappa\{2I_zS_z(x,\gamma)+2I_yS_y(x,\gamma)\}$. The remaining τ, prepares the effective Hamiltonian $\kappa\{2I_zS_z(x,\gamma)-2I_yS_y(x,\gamma)\}$, resulting in a total evolution given by $H_p(\frac{\pi}{2}) = \frac{\pi}{2}(2I_zS_z(x,\gamma))$.

Choosing $p-q=-1$ and $p,q>2$ for the whole duration prepares the effective Hamiltonian

$$H_{dcp} = \kappa\{I_zS_z(x,\gamma)+I_yS_y(x,\gamma)\}, \tag{4}$$

Let $H_{dcp}(\pi) = \pi(I_zS_z(x,\gamma)+I_yS_y(x,\gamma))$, correspond to a π rotation under H_{dcp}, respectively.

The effective Hamiltonian H_{dcp} mediates the coherence transfer $I_x \to S_x$ with an efficiency independent of the γ Euler angle. However, the effective Hamiltonian H_{dcp} does not transfer both components of the transverse magnetization, i.e., $S_x + iS_y \to I_x + iI_y$. We now show how both components of the transverse magnetization of spin S can be transferred by suitably preparing the initial state by the preparation Hamiltonian H_p. The preparation involves evolving the initial magnetization S_x under $H_p(\pi/2)$. In the interaction frame of the rf-irradiation

$$S_x \xrightarrow{H_p(\pi/2)} 2I_zS_y(x,\gamma). \tag{5}$$

In the original double rotating Zeeman frame, the state takes the form

$$\exp(-i\theta_S S_x)2I_zS_y(x,\gamma)\exp(i\theta_S S_x) = 2I_zS_y(x,\gamma+\theta_S),$$

where $\theta_S = 2\tau\omega_{rf}^S$.

Now consider the following sequence of transformations

Experiment A

$$\begin{aligned} S_x &\xrightarrow[\text{I}]{H_p(\pi/2)} 2I_zS_y(x,\gamma+\theta_S) \xrightarrow[\text{II}]{(\frac{\pi}{2})_y^S} 2I_zS_y(\bar{z},\gamma+\theta_S) \\ &\times \xrightarrow[\text{III}]{\omega_s S_z} 2I_zS_y(\bar{z},\gamma+\theta_S-\omega_S t_1) \xrightarrow[\text{IV}]{(\frac{\pi}{2})_{\bar{y}}^{I,S}} \\ &- 2I_xS_y(x,\gamma+\theta_S-\omega_s t_1) \xrightarrow[\text{V}]{H_{dcp}(\pi)} I_z(x,\theta_S+\theta_I-\omega_S t_1) \\ &\times \xrightarrow[\text{VI}]{(\frac{\pi}{2})_{\bar{y}}^{I}} I_x(z,\omega_s t_1-\theta_I-\theta_S). \end{aligned} \tag{6}$$

Here $\theta_I = 2\tau\omega_{rf}^I$, where 2τ is the time to synthesize $H_{dcp}(\pi)$. The precession of spin I is now recorded during the t_2 evolution period. The pulse sequence for the experiment is depicted in Fig. 1(A).

Remark 2. In absence of rf-inhomogeneity, the phases θ_S and θ_I remain the same for the whole sample for all t_1 increments. When the time τ is an integral number of rotor periods, these phases are simply factors of 2π. However in the presence of the inhomogeneity of the rf-field, these phase factors will show variation across the sample, leading to reduction in the sensitivity in the experiments. In Section 4, we show how the defocussing of the phases in the presence of inhomogeneity can be refocussed.

Remark 3. In the above analysis, we have neglected the dispersion in κ (caused due to dispersion in β) and assumed a nominal value κ_0. The period for the DCP experiment was chosen based on a nominal value of κ_0. In Section 4, we address the problem of compensation of κ. There is significant literature on use of adiabatic sequences for compensating dispersion in the value of κ [17]. In our recent work, we have shown [12] that dispersion in κ can also be compensated by using ideas of composite pulse sequences from Liquid state NMR [13] and methods of optimal control [14]. In Section 4, we show how adiabatic sequences and optimal control methods can be incorporated for compensating dispersion in κ in the sensitivity enhanced experiments presented here.

In the above experiment, we started from magnetization on spin S and collected the chemical shift information of spin S during the t_1 evolution, followed by transfer of magnetization to spin I and detection of spin I. We now show how to start from the initial magnetization on spin I and encode it in such a way so that we collect chemical shift information of spin S during the t_1 evolution and finally detect on spin I. The various steps are summarized as follows.

Experiment B

$$\begin{aligned} I_z &\xrightarrow[\text{I}]{H_{dcp}(\pi)} 2I_xS_y(x,\gamma+\theta_S) \xrightarrow[\text{II}]{(\frac{\pi}{2})_y^{I,S}} 2I_zS_y(z,\gamma+\theta_S) \xrightarrow[\text{III}]{\omega_s S_z} \\ &2I_zS_y(z,\gamma+\omega_s t_1+\theta_S) \xrightarrow[\text{IV}]{(\frac{\pi}{2})_y^{I,S}} 2I_xS_y(x,\gamma+\omega_s t_1+\theta_S) \xrightarrow[\text{V}]{H_{dcp}(\pi)} \\ &- I_z(x,\omega_s t_1+\theta_S+\theta_I) \xrightarrow[\text{VI}]{(\frac{\pi}{2})_{\bar{y}}^{I}} I_x(z,\omega_s t_1+\theta_I+\theta_S). \end{aligned} \tag{7}$$

Here steps I and II constitute the preparation period and step III is the chemical shift evolution for spin S for t_1 units of time. Again θ_I and θ_S are $2\tau\omega_{rf}^I$ and $2\tau\omega_{rf}^S$, respectively, where 2τ as before is the DCP evolution period. As remarked earlier, in the absence of rf-inhomogeneity, the additional phases θ_I and θ_S are constant over the whole sample. In the presence of inhomogeneity, the dispersion of these phases will lead to loss of sensitivity. Methods to refocus this dispersion is described in Section 4. The pulse sequences for the transformations in Eq. (7) are shown in the Fig. 1(B).

3. Homonuclear spins

We now extend these ideas to design of sensitivity enhanced experiments for homonuclear spin systems. Consider two dipolar coupled homonuclear spins I and S for which the MAS modulated dipolar-coupling Hamiltonian is of the form

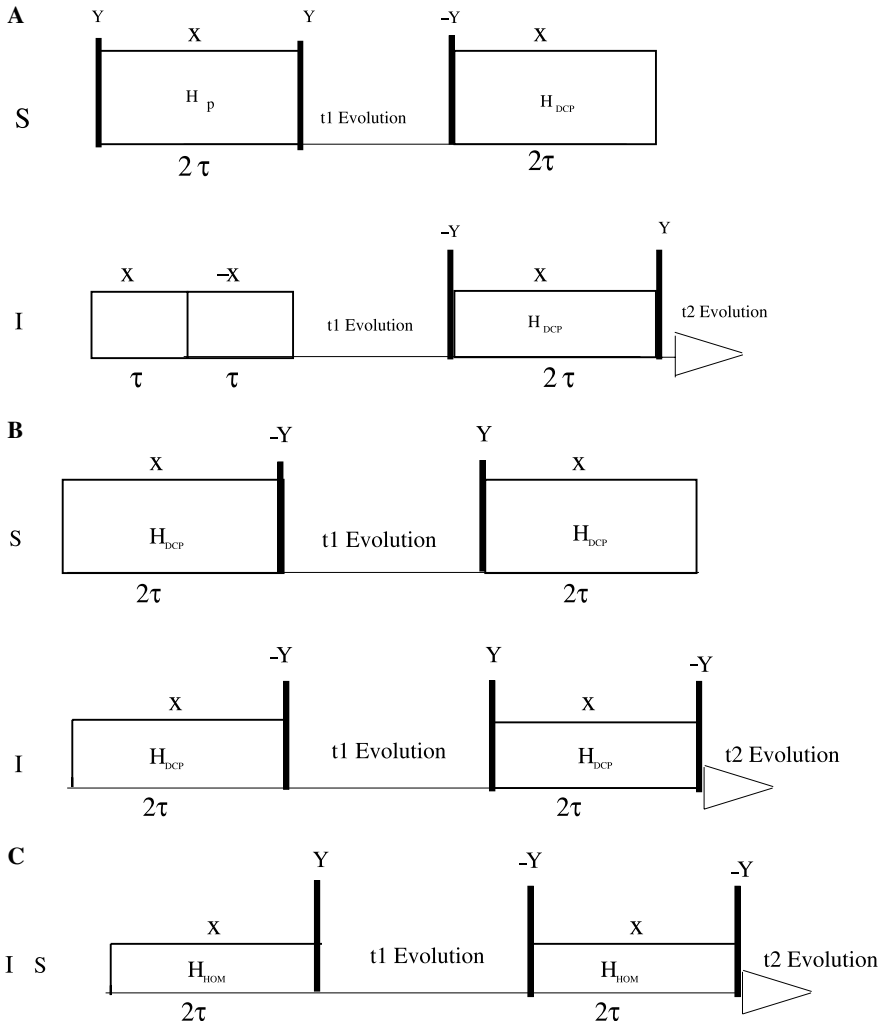

Fig. 1. In figure (A), the starting operator is S_z. The H_p block corresponds to x phase irradiation on spin S and I with amplitude $\omega_{rf}^I = p\omega_r$ and $\omega_{rf}^S = q\omega_r$ for time $\tau = \frac{\pi}{2\kappa_0}$, followed by $\omega_{rf}^I = -p\omega_r$ and $\omega_{rf}^S = q\omega_r$ for time $\tau = \frac{\pi}{2\kappa_0}$. The H_{dcp} block is prepared by x phase irradiation on I and S spin for duration $2\tau = \frac{\pi}{\kappa_0}$, with $\omega_{rf}^I = p\omega_r$ and $\omega_{rf}^S = q\omega_r$. Here $p - q = -1$ and $p, q > 2$. In figure (B), the starting operator is I_z. The effective Hamiltonian H_{dcp} is prepared as before. In figure (C), the starting operator is I_z. The effective Hamiltonian H_{hom} is prepared by x phase irradiation on I and S spin for duration $2\tau = \frac{\pi}{\kappa_0}$, with $\omega_{rf}^I = \frac{\omega_r}{2}$ and $\omega_{rf}^S = \frac{\omega_r}{2}$. All solid dark bars represent $\frac{\pi}{2}$ hard pulses.

$$H_{IS}(t) = \omega_{IS}(t)(\mathbf{I}.\mathbf{S} - 3I_zS_z). \tag{8}$$

In the interaction frame of a non-selective constant-phase rf irradiation, the $\omega_{IS}(t)\mathbf{I}.\mathbf{S}$ component averages to zero over a rotor period as the operator term $\mathbf{I}.\mathbf{S}$ commutes with the rf Hamiltonian (e.g., $I_x + S_x$). This leaves us with the modulation of the $3I_zS_z$ component, and a formalism very similar to that described above for the heteronuclear case applies. The only difference is that one has non-selective rf irradiation. The two spins are irradiated at their mean resonance frequency by a rf field with the amplitude ω_{rf} adjusted to half the rotor frequency, i.e., $\omega_{rf} = \frac{1}{2}\omega_r$ [15]. Using Eq. (2) with $p = q = \frac{1}{2}$, the dipolar coupling Hamiltonian in the interaction frame of the rf-irradiation averages over a rotor period to

$$H_{hom} = \kappa[\cos(\gamma)(I_zS_z - I_yS_y) - \sin(\gamma)(I_zS_y + I_yS_z)], \tag{9}$$

with $\kappa = \frac{3}{4\sqrt{2}} b_{IS} \sin(2\beta)$. Which we re-write as

$$H_{hom} = \kappa[I_zS_z(x,\gamma) - I_yS_y(x,\gamma)].$$

Finally letting H_{hom} evolve for $\frac{\pi}{\kappa_0}$, prepares

$$H_{hom}(\pi) = \pi\{I_zS_z(x,\gamma) - I_yS_y(x,\gamma)\}.$$

Starting from the initial state I_z, we perform the following sequence of transformations,

Experiment C

$$I_z \xrightarrow[\text{I}]{H_{hom}(\pi)} -2I_xS_y(x,\gamma+\theta) \xrightarrow[\text{II}]{(\frac{\pi}{2})_y} 2I_zS_y(\bar{z},\gamma+\theta) \xrightarrow[\text{III}]{\omega_sS_z} 2I_zS_y$$
$$(\bar{z},\gamma-\omega_st_1+\theta) \xrightarrow[\text{IV}]{(\frac{\pi}{2})_{\bar{y}}} -2I_xS_y(x,\gamma-\omega_st_1+\theta) \xrightarrow[\text{V}]{H_{hom}(\pi)}$$
$$-I_z\cos(\omega_st_1) + I_y\sin(\omega_st_1) \xrightarrow[\text{VI}]{(\frac{\pi}{2})_{\bar{y}}} I_x(z,\omega_st_1).$$

As before, steps I and II constitute the preparation phase and III, the evolution of chemical shift for spin S for time

t_1. Also note that the phase θ finally gets eliminated. The pulse sequence for the experiment is presented in Fig. 1(C).

Remark 4 (*Triple resonance experiments*)**.** These sensitivity enhanced techniques can be extended to the design of multidimensional experiments. Consider again the coupled homonuclear *IS* spin system. This could for example represent CACX pair or COCX moeity in the triple resonance NCACX and NCOCX experiments [16]. We start with an initial coherence on spin I, given by $I_x\cos(\delta) + I_y\sin(\delta)$. The phase δ encodes the chemical shift information of the third spin of interest, say ^{15}N in [16]. The initial state $I_x(z,\delta)$ is transformed under the following steps

$$I_x(z,\delta) \xrightarrow[\text{I}]{(\frac{\pi}{2})_{\bar{y}}} I_z(x,-\delta) \xrightarrow[\text{II}]{H_{\text{hom}}(\pi)} -2I_xS_y(x,\gamma+\theta-\delta) \xrightarrow[\text{III}]{(\frac{\pi}{2})_y} 2I_zS_y$$
$$(\bar{z},\gamma+\theta-\delta) \rightarrow \xrightarrow[\text{IV}]{\omega_s S_z} 2I_zS_y(\bar{z},\gamma+\theta-\delta-\omega_s t_1) \xrightarrow[\text{V}]{(\frac{\pi}{2})_{\bar{y}}} -2I_xS_y$$
$$(x,\gamma+\theta-\omega_s t_1-\delta) \xrightarrow[\text{VI}]{H_{\text{hom}}(\pi)} I_x(z,\omega_s t_1+\delta).$$

The precession of the spin I can now be recorded.

4. Adiabatic pulses for compensating rf-inhomogeneity and dispersion in κ

Until now we have neglected inhomogeneity in the rf-field and dispersion in the value of κ. Now we show that by use of adiabatic pulses, it is possible to compensate for these anisotropies and at the same time transfer both components of transverse magnetization spin S onto spin I during the mixing period. To illustrate the main ideas, we first start with the case of homonuclear spins.

Consider again coupled homonuclear spins which are irradiated with rf field strength of $\omega_{\text{rf}}(t) = \frac{\omega_r+u(t)}{2}$. Let $F_x^- = \frac{I_x-S_x}{2}$ and $F_x^+ = \frac{I_x+S_x}{2}$. In the interaction frame of x phase rf-irradiation of strength $\frac{\omega_r}{2}$, the Hamiltonian averages to

$$H_{\text{hom}}(t) = \kappa\{I_zS_z(x,\gamma) - I_yS_y(x,\gamma)\} + ((1+\epsilon)u(t) + \epsilon\omega_r)\frac{F_x^+}{2}, \tag{10}$$

where $0 < \epsilon < 1$ represents the inhomogeneity of the field. Let $A \gg \kappa$ and $A \gg \epsilon_{\max}\omega_r$. Now if the field $u(t)$, in the time τ_a, is swept adiabatically from a value A to $-A$, then the initial operator, $F_x^+ \rightarrow -F_x^+$ for a broad range of κ and ϵ. This range depends on A and the sweep rate. This represents the standard adiabatic passage in the double quantum frame. Such adiabatic sweeps have been well explored and are widely used [17,18]. The resulting unitary propagator generated by evolution of $H_{\text{hom}}(t)$ can then be written as

$$U = \exp(-i\phi_0F_x^+)\exp(-i\pi(I_zS_z(x,\gamma) - I_yS_y(x,\gamma))) \times \exp(i\phi_2F_x^+).$$

Here ϕ_0 and ϕ_2, depend on κ and ϵ. In the original Zeeman frame, the net evolution takes the form $U_1 = \exp(-i\theta F_x^+)U$, where $\theta = \frac{\tau_a\omega_r}{2}$. This simply modifies ϕ_0 in the expression for U to ϕ_1. We then rewrite

$$U_1 = \exp(-i\phi_1F_x^+)\exp(-i\pi(I_zS_z(x,\gamma) - I_yS_y(x,\gamma))) \times \exp(i\phi_2F_x^+).$$

Consider now the following sequence of transformations,

Experiment D

$$I_z \xrightarrow[\text{I}]{U_1} -2I_xS_y(x,\gamma+\phi_1+\phi_2) \xrightarrow[\text{II}]{(\frac{\pi}{2})_y} 2I_zS_y(\bar{z},\gamma+\phi_1+\phi_2) \times \xrightarrow[\text{III}]{\omega_s S_z} 2I_zS_y(\bar{z},\gamma+\phi_1+\phi_2-\omega_s t_1) \xrightarrow[\text{IV}]{(\frac{\pi}{2})_{\bar{y}}} -2I_xS_y(x,\gamma+\phi_1+\phi_2-\omega_s t_1) \xrightarrow[\text{V}]{U_1} -I_z\cos(\omega_s t_1) + I_y\sin(\omega_s t_1) \xrightarrow[\text{VI}]{(\frac{\pi}{2})_{\bar{y}}} I_x(z,\omega_s t_1).$$

This experiment is a modified version of Experiment C, where steps I and V in Experiment C have been replaced by adiabatic pulse sequences, making the original experiment robust to inhomogeneities in the strength of the rf-field and dispersion in value κ. Adiabatic sequences tend to be long. In our recent work, using ideas of optimal control, we have developed sequences that are shorter than adiabatic sequences and give comparable compensation [12]. We can replace the adiabatic sweeps in Experiment D, by these optimal control pulse sequences and obtain shorter experiments that are sensitivity enhanced and still robust to inhomogeneities in strength of the rf-field and dispersion κ.

We now consider the case of Heteronuclear spins I and S, as in Experiment B. The spins are irradiated with rf field strength of $\omega_{\text{rf}}^I(t) = p\omega_r$ and $\omega_{\text{rf}}^S(t) = q\omega_r$, such that $p - q = -1$ and $p, q > 2$. Let $\Delta\omega_{\text{rf}}^I$ and $\Delta\omega_{\text{rf}}^S$ represent the dispersion in the I- and S-spin rf field strengths from their nominal values $p\omega_r$ and $q\omega_r$, respectively. Let $\Delta\omega_{\text{rf}}^{\pm} = (\Delta\omega_{\text{rf}}^I \pm \Delta\omega_{\text{rf}}^S)$. In the interaction frame of rf-irradiation, the Hamiltonian averages to

$$H_{\text{dcp}} + \Delta\omega_{\text{rf}}^+F_x^+ + \Delta\omega_{\text{rf}}^-F_x^-. \tag{11}$$

Now if we apply an additional x field on say spin I with time varying rf-strength $u(t)$, we obtain a time varying Hamiltonian

$$H_{\text{dcp}} + (\Delta\omega_{\text{rf}}^+ + \epsilon u(t))F_x^+ + (\Delta\omega_{\text{rf}}^- + \epsilon u(t))F_x^-. \tag{12}$$

Note $\frac{I_x+S_x}{2}$ commutes with H_{dcp}. Now if the field $u(t)$, in time τ_a, is swept adiabatically from a value A ($\gg \kappa, \Delta\omega_{\text{rf}}^-$) to $-A$, then the initial operator, F_x^- is inverted, i.e., $F_x^- \rightarrow -F_x^-$ for a broad range of κ and ϵ (the range depends on A and the sweep rate). This is the standard adiabatic passage in the zero quantum frame. The resulting unitary transformation can be denoted by

$$W(\gamma) = \exp(i\phi_1F_x^-)\exp(-i\pi(I_zS_z(x,\gamma) + I_yS_y(x,\gamma))) \times \exp(-i\phi_2F_x^-)\exp(-i\phi_3F_x^+).$$

where ϕ_1 and ϕ_2 depend on κ and ϵ and ϕ_3 depends on ϵ.

If we irradiate spins I and S with $-x$ phase rf-field strengths of $\omega_{\text{rf}}^I(t) = q\omega_r$ and $\omega_{\text{rf}}^S(t) = p\omega_r + u(t)$ for

duration τ_a, with p, q, τ_a and $u(t)$ as described above. Then (assuming same rf-inhomogeneity on both the channels), we prepare the propagator,

$$W_1(\gamma) = \exp(i\phi_1 F_x^-) \exp(-i\pi(I_z S_z(x,\gamma) + I_y S_y(x,\gamma))) \times \exp(-i\phi_2 F_x^-) \exp(i\phi_3 F_x^+).$$

Now we consider the following experiment

Experiment E

$$I_z \xrightarrow[\text{I}]{W} 2I_x S_y(x, \gamma+\phi_1+\phi_2+\phi_3) \xrightarrow[\text{II}]{(\frac{\pi}{2})_y^{I,S}} -2I_z S_y(\bar{z}, \gamma+\phi_1+\phi_2+\phi_3) \xrightarrow[\text{III}]{\omega_s S_z} -2I_z S_y(\bar{z}, \gamma+\phi_1+\phi_2+\phi_3-\omega_s t_1) \xrightarrow[\text{IV}]{(\frac{\pi}{2})_y^{I,S}} 2I_x S_y(x, \gamma+\phi_1+\phi_2+\phi_3-\omega_s t_1) \xrightarrow[\text{V}]{W_1} I_z(x, -\omega_s t_1) \xrightarrow[\text{VI}]{(\frac{\pi}{2})_y^{I}} I_x(z, \omega_s t_1).$$

The step I of the experiment constitutes the preparation step before the t_1 evolution and step V constitutes the transfer step.

Once again for practical concerns of relaxation, one might want to reduce the length of the experiment and replace the adiabatic sequences used in steps I and V by simply a ramped DCP experiment or an optimal control experiment as presented in [12]. One simply has to observe the relation that $\omega_{rf}^I(t)$ and $\omega_{rf}^S(t)$ used in the step I is replaced by $-\omega_{rf}^S(t)$ and $-\omega_{rf}^I(t)$ in the step V of the experiment (assuming same inhomogeneity on both rf-channels) (Fig. 2).

Remark 5. We have chosen the DCP and HORROR experiments as prototype of heteronuclear and homonuclear re-coupling experiments. However, the framework of using two recoupling periods and creation of γ dependent antiphase polarization during t_1 evolution is more general. It allows for incorporation of more advanced re-coupling sequences [24–28] that provide robust performance in presence of large chemical shift dispersion. In our future work, we plan to incorporate these superior sequences in the two re-coupling periods.

Remark 6. The coupled heteronuclear spin pair *IS* discussed here in practical applications could correspond to ^{13}C and ^{15}N, respectively. Similarly the homonuclear spin pair discussed here correspond to ^{13}C–^{13}C correlation experiments. In both the experiments, the proton bath needs to be be decoupled from the spin system. This can be achieved by TPPM sequences [20] during the t_1 and t_2 evolution period and CW radiation on protons during the preparation and transfer phase of these experiments.

5. Results and simulations

Powder averaged numerical simulations were performed for simple two-spin heteronuclear and homonuclear systems to verify and quantify the sensitivity enhancement results expected from preservation of both transverse components in the t_1-dimension. All simulations were performed using the SPINEVOLUTION software [29]. For powder averaging, a comprehensive compilation of various angle sets from the literature [30,31] is provided with the SPINEVOLUTION program. Simulations were performed using one of these angle sets which averages over 232 differ-

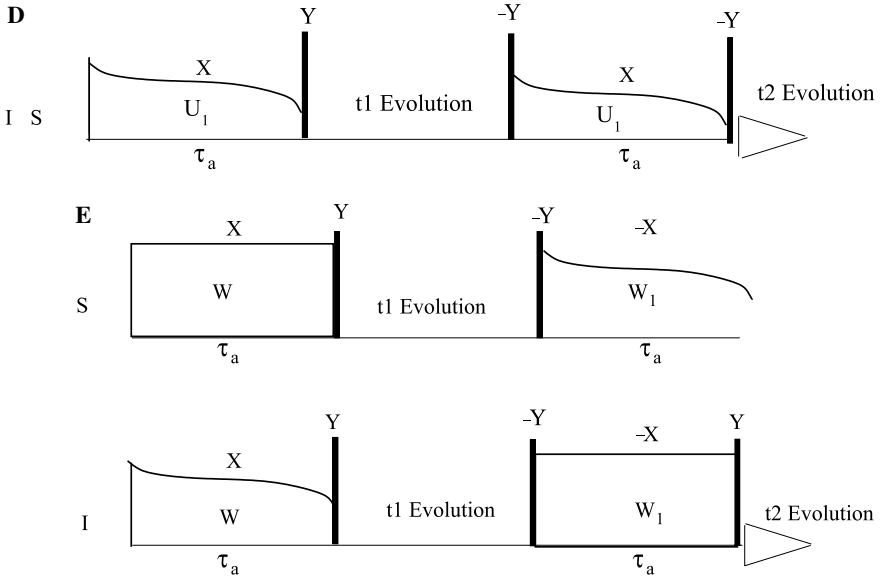

Fig. 2. In figure (D), the starting operator is I_z. The effective propagotor U_1 is prepared by x phase irradiation on I and S spin for duration τ_a, with $\omega_{rf}(t) = \frac{\omega_r + u(t)}{2}$, where $u(t)$ is swept adiabatically from A to $-A$. In figure 2(E), the starting operator is I_z. The propagator W is prepared by x phase irradiation on I and S with $\omega_{rf}^I(t) = p\omega_r + u(t)$ and $\omega_{rf}^S = q\omega_r$ such that $p - q = -1$, $|p + q| > 2$, and $u(t)$ is swept adiabatically from A to $-A$. The propagator W_1 is prepared by $-x$ phase irradiation on I and S, such that $\omega_{rf}^I(t) = q\omega_r$, $\omega_{rf}^S = p\omega_r + u(t)$ with p, q and $u(t)$ as before.

ent (α, β) angles. Addition averaging was performed over 20 different γ angles. Simulations were performed for both adiabatic and nonadiabatic pulse sequences. All spectra shown subsequently are obtained by taking 128 points in the t_1 dimension with an increment of 100 μs. The t_1 increments are chosen to be integral number of rotor periods.

For heteronulear experiment, we first simulated the efficiency of a typical $^{15}N \rightarrow {}^{13}C$ coherence transfer using the standard DCP experiment [11]. Our calculations addressed the well characterized [19] $^{13}C_\alpha$–^{15}N spin pair of glycine in a powder sample subject to 10 kHz MAS, an external magnetic field corresponding to a 700 MHz (Larmor frequency for ^1H) spectrometer, and nominal rf-field strength on the ^{13}C and ^{15}N channels of 35 and 45 kHz, respectively. Fig. 3, (left panel) shows the efficiency of coherence transfer $^{15}N \rightarrow {}^{13}C$ as a function of the mixing time τ_d. The optimal mixing time of $\tau_d^* = 2$ ms corresponding to the maximum efficiency of ≈73% is recorded from this plot and used subsequently in experiments A and B. Experiment A is simulated with $2\tau = \tau_d^*$ and by incrementing the indirect evolution time t_1. After the transfer, the density matrix $\rho(t_1, t_2)$ is a function of the variables t_1 and t_2. In Fig. 4B, we display the spectrum obtained by taking the magnitude of the Fourier transform of $\langle I^+ \rangle(t_1) = \mathrm{tr}(\rho(t_1, 0) I^+)$. We take the magnitude to quantify the total polarization transferred to spin I after t_1 evolution. In Fig. 4A is shown the analogous spectrum obtained by using the standard DCP transfer block (transfer time τ_d^*) after the t_1 evolution. Both spectra (and all subsequent spectra) are obtained by taking 128 points in the t_1 dimension with an increment of 100 μs. The doublet in the Fig. 4A results from the fact that the transferred x component of spin S is modulated as $\cos(\omega_s t_1)$ and the resulting spectrum has peaks at ω_s and $-\omega_s$. Although not customary, we show the doublet to highlight the $\cos(\omega_s t_1)$ modulation when only one component is transferred after t_1 evolution. The ratio of the peak amplitudes of spectra B to A is 2.0. This corresponds to sensitivity enhancement of experiment A over standard DCP experiment by a factor $\sqrt{2}$.

Fig. 5 shows simulated spectra for experiments B and E. Spectrum in Fig. 5A is identical to one in Fig. 4A and is obtained by using the standard DCP transfer block (transfer time τ_d^*) after the t_1 evolution. Spectrum in Fig. 5C is obtained by use of adiabatic pulses in the DCP transfer [17]. Spectrum in Fig. 5B was obtained by transferring both components after t_1 evolution as in Experiment B. The magnetization is initially transferred from ^{13}C during the first recoupling period and after collecting the chemical shift of ^{15}N, it is transferred back. The mixing time in Experiment B is chosen to be $2\tau = \tau_d^*$. Spectrum in Fig. 5D is the adiabatic version of this experiment (Experiment E). Adiabatic pulses used in simulating spectrum C and D were of duration $10\tau_d^*$. The ratio of the peak amplitudes of spectra $A{:}B{:}C{:}D = 1{:}1.9{:}1.2{:}2.15$. All spectra were obtained by taking 128 points in the t_1 dimension with an increment of 100 μs.

Remark 7. In experiments B and E, for small κ values, the first recoupling period will not generate complete antiphase polarization. The left over or residual inphase magnetization on spin I will evolve at frequency ω_I during the t_1 period. The second recoupling period also leaves some part of this magnetization back on spin I. As a result there is polarization on spin I after the two recoupling periods, which has evolved at frequency ω_I rather than ω_s during the t_1 period. We have not shown here the distinct peak in the spectrum arising due to this left over magnetization. The same phenomenon occurs in homonuclear recoupling experiments

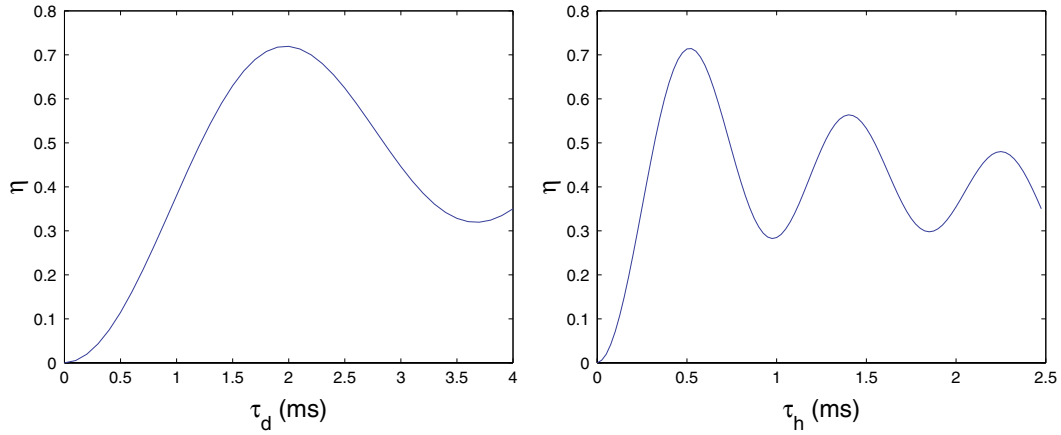

Fig. 3. Left panel shows efficiency η of $^{15}N \rightarrow {}^{13}C$, coherence transfer for the DCP experiment as a function of the mixing time τ_d, with experimental conditions corresponding to MAS experiments with 10 kHz spinning and using a 700 MHz (Larmor frequency of ^1H) magnet. The nominal rf-field strength of $\omega_{rf}^C/2\pi = 35$ kHz and $\omega_{rf}^N/2\pi = 45$ kHz were used. The calculations used $\delta_{iso}^C = 0$, $\delta_{aniso}^C = 19.43$ ppm, $\eta^C = .98$, $\{\alpha_{PR}^C, \beta_{PR}^C, \gamma_{PR}^C\} = \{64.9^\circ, 37.3^\circ, -28.8^\circ\}$, $\delta_{iso}^N = 10$, $\delta_{aniso}^N = 10.1$ ppm, $\eta^N = 0.17$, $\{\alpha_{PR}^N, \beta_{PR}^N, \gamma_{PR}^N\} = \{-83.8^\circ, -79.0^\circ, 0.0^\circ\}$, and internuclear distance $r_{CN} = 1.52$Å, $\{\alpha_{PR}^{CN}, \beta_{PR}^{CN}, \gamma_{PR}^{CN}\} = \{0^\circ, 0^\circ, 0^\circ\}$, and $J_{CN} = -11$ Hz. Right panel shows calculated efficiency of $^{13}C \rightarrow {}^{13}C$, coherence transfer for the HORROR experiment as a function of the mixing time τ_h, with experimental conditions corresponding to MAS experiments with 20 kHz spinning and using a 700 MHz (Larmor frequency of ^1H) magnet. The nominal rf-field strength of $\omega_{rf}^C/2\pi = 10$ kHz. The calculations used internuclear distance $r_{CN} = 1.52$Å between the carbon pairs under ideal conditions $\delta_{aniso}^I = \eta^I = \delta_{aniso}^S = \eta^S = 0$ and $\delta_{iso}^I = 0$ and $\delta_{iso}^S = 10$ ppm.

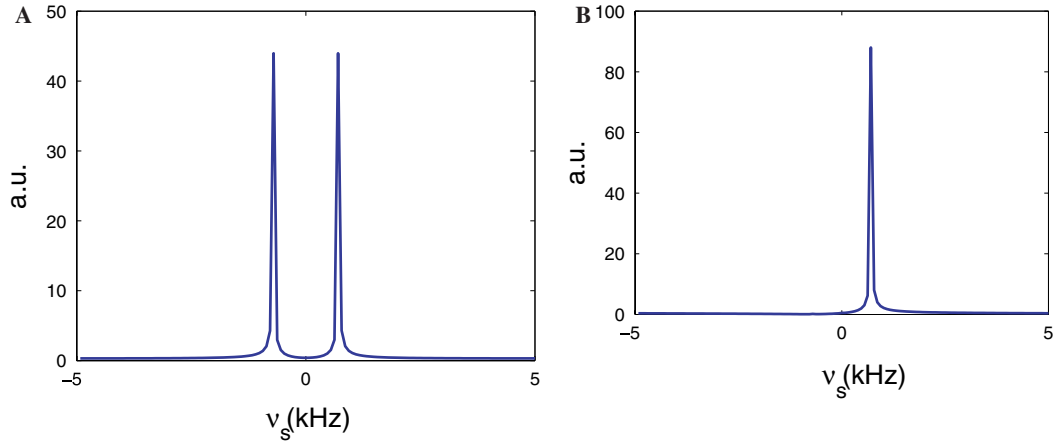

Fig. 4. Numerical simulations for the DCP experiment (A) and the sensitivity enhanced experiment A (B), using the $^{13}C_\alpha$–^{15}N spin pair of glycine in a powder sample subject to 10 kHz MAS, an external magnetic field corresponding to a 700 MHz (Larmor frequency for ^1H) spectrometer. The nominal rf-field strength of $\omega_{rf}^C/(2\pi) = 35$ kHz and $\omega_{rf}^N/(2\pi) = 45$ kHz were used. The ratio of the peak amplitudes of spectrum B to A is 2.0. The doublet in Fig. A arises from the $\cos(\omega_s t_1)$ modulation of transferred x component of spin S.

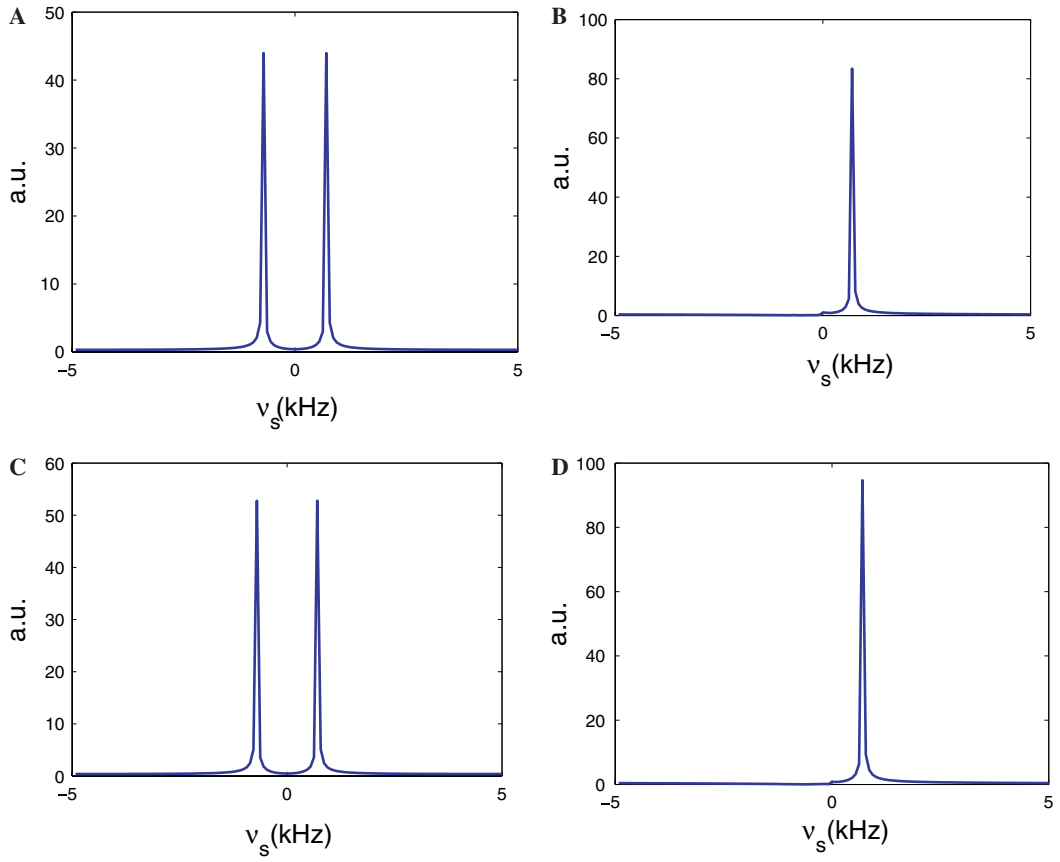

Fig. 5. Numerical simulations for the DCP experiment (A) and the sensitivity enhanced experiment B (B), using the $^{13}C_\alpha$–^{15}N spin pair of glycine in a powder sample subject to 10 kHz MAS, an external magnetic field corresponding to a 700 MHz (Larmor frequency for ^1H) spectrometer. The nominal rf-field strength of $\omega_{rf}^C/2\pi = 35$ kHz and $\omega_{rf}^C/2\pi = 45$ kHz were used in the DCP experiment and experiment B. The S spin is represented by ^{15}N and the I spin is represented by $^{13}C_\alpha$. Spectra C and D correspond to adiabatic versions of experiments A and B. The duration of adiabatic sequences was chosen to be $10\tau_d^*$. The ratio of the peak amplitudes of spectra $A{:}B{:}C{:}D = 1{:}1.9{:}1.2{:}2.15$.

For homonuclear experiments, we chose as our model system the ^{13}C–^{13}C spin-pair (under ideal conditions) in a powder sample subject to 20 kHz MAS, an external magnetic field corresponding to a 700 MHz (Larmor frequency for ^1H) spectrometer, and nominal rf-field strength on the ^{13}C channel of 10 kHz. Fig. 3(right panel) shows the

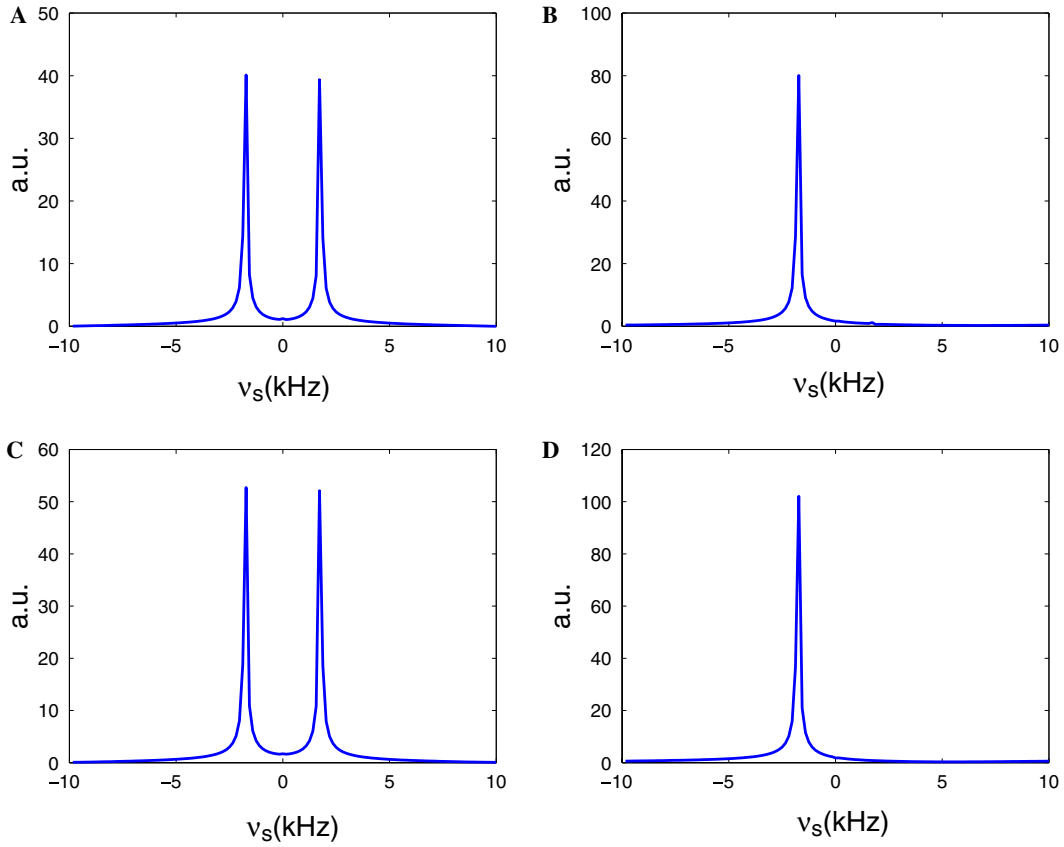

Fig. 6. Numerical simulation for the ^{13}C–^{13}C spin-pair in a powder sample subject to 20 kHz MAS, an external magnetic field corresponding to a 700 MHz (Larmor frequency for ^{1}H) spectrometer, and nominal rf-field strength on the ^{13}C channel of 10 kHz. Spectra A and C are obtained from standard HORROR experiment and its adiabatic version, respectively. The mixing time of $\tau_h^* = 0.525$ ms corresponding to the maximum efficiency is used in the HORROR experiment [15]. The length of adiabatic sequences were chosen to be $20\tau_h^*$. Experiment C is simulated with $2\tau = \tau_h^*$. Spectra in panel B and D correspond to experiments C and D, respectively. The ratio of the peak amplitudes of spectra $A{:}B{:}C{:}D = 1{:}2.0{:}1.31{:}2.55$.

coherence transfer efficiency as as function of the mixing time τ_h in the standard HORROR experiment [15]. The optimal mixing time of $\tau_h^* = 0.525$ ms corresponding to the maximum efficiency of $\approx 73\%$ is used subsequently. Experiment C is simulated with $2\tau = \tau_h^*$ and by incrementing the indirect evolution time t_1. After the transfer, the density matrix $\rho(t_1, t_2)$ is a function of variable t_1 and t_2. The spectrum obtained by taking the magnitude of the Fourier transform of $\langle I^+ \rangle(t_1) = \mathrm{tr}(\rho(t_1, 0), I^+)$ is displayed in 6B. Fig. 6A is obtained by using the standard HORROR transfer block (transfer time τ_h^*) after the t_1 evolution. Spectra in Figs. 6C and D correspond to numerical simulations of adiabatic versions of experiments A and B, respectively. The length of adiabatic sequences were chosen to be $20\tau_h^*$. The ratio of the peak amplitudes of spectra $A{:}B{:}C{:}D = 1{:}2.0{:}1.31{:}2.55$.

5.1. Discussion and conclusion

In this paper, we introduced 2D NMR experiments under MAS, which use evolution of γ dependent anti-phase coherences during the t_1 evolution period. Unlike standard 2D recoupling experiments, this technique uses two recoupling periods. The first recoupling period is used to create γ dependent anti-phase coherence. The second recoupling period transfers both components of this anti-phase coherence to the coupled spin, following the t_1 evolution period. In the absence of relaxation losses this results in sensitivity enhancement by a factor of $\sqrt{2}$, in 2D NMR experiments over standard methods which only transfer say the x component of the transverse magnetization. We then showed that by use of adiabatic pulses in the recoupling periods, the experiments can be made robust to inhomogeneties and anisotropies. We verified the expected gains using numerical simulations on model heteronuclear and homonuclear two spin systems. The implementation of the experiments proposed in this paper is straightforward. It is expected that experiments based on the principle of γ preparation might be widely used in MAS Solid State NMR applications.

Acknowledgment

The work was supported by ONR 38A-1077404, AFOSR FA9550-05-1-0443 and AFOSR FA9550-04-1-0427.

References

[1] S.J. Opella, Nat. Struct. Biol. 4 (1997) 845–848.
[2] R.G. Griffin, Nat. Struct. Biol. 5 (1998) 508–512.
[3] F. Castellani, B. van Rossum, A. Diehl, M. Schubert, K. Rehbein, H. Oschkinat, Nature 420 (2002) 98–102.
[4] A.T. Petkova, Y. Ishii, J.J. Balbach, O.N. Antzutkin, R.D. Leapman, F. Deglaglio, R. Tycko, Proc. Natl. Acad. Sci. 99 (2002) 16742–16747.
[5] C.P. Jaroniec, C.E. MacPhee, V.S. Baja, M.T. McMahon, C.M. Dobson, R.G. Griffin, Proc. Natl. Acad. Sci. 101 (2004) 711–716.
[6] A.G. Palmer III, J. Cavanagh, P.E. Wright, M. Rance, Proc. Natl. Acad. Sci. 93 (1991) 151;
L.E. Kay, J. Am. Chem. Soc. 115 (1993) 2055;
M. Sattler, P. Schmidt, J. Schleucher, O. Schedletzky, S.J. Glaser, C. Griesinger, J. Magn. Reson. B 108 (1995) 235;
J. Schleucher, M. Schwendinger, M. Sattler, P. Schmidt, O. Schedletzky, S.J. Glaser, O.W. Sørensen, C. Griesinger, J. Biomol. NMR 4 (1994) 30.
[7] R. Tycko, ChemPhysChem 5 (2004) 863–868.
[8] R.R. Ernst, G. Bodenhausen, A. Wokaun, Principles of Nuclear Magnetic Resonance in One and Two Dimensions, Clarendon Press, Oxford, 1987.
[9] M. Bak, J.T. Rasmussen, N.C. Nielsen, J. Magn. Reson. 147 (2000) 296–330.
[10] M. Bjerring, J.T. Rasmussen, R.S. Krogshave, N.C. Nielsen, J. Chem. Phys. 119 (2003) 8916–8926.
[11] J. Schaefer, R.A. McKay, E.O. Stejskal, J. Magn. Reson. 34 (1979) 443–447.
[12] N. Khaneja, C. Kehlet, S.J. Glaser, N.C. Nielsen, J. Chem. Phys. 124 (2006) 114503.
[13] M.H. Levitt, Prog. NMR Spectrosc. 18 (1986) 61–122.
[14] N. Khaneja, T. Reiss, C. Kehlet, T. Schulte-Herbruggen, S.J. Glaser, J. Magn. Reson. 172 (2005) 296–305.
[15] N.C. Nielsen, H. Bildsøe, H.J. Jakobsen, M.H. Levitt, J. Chem. Phys. 101 (1994) 1805–1812.
[16] J. Pauli, M. Baldus, B. Rossum, H. Groot, H. Oschkinat, ChemBioChem 2 (2001) 272–281.
[17] M. Ernst, B.H. Meier, Encyclopedia of NMR 9 (2002) 23–32.
[18] R. Verel, M. Ernst, B.H. Meier, J. Mag. Reson. 150 (1) (2001) 81–99.
[19] L. Odgaard, M. Bak, H.J. Jakobsen, N.C. Nielsen, J. Magn. Reson. 148 (2001) 298.
[20] A.E. Bennett, C.M. Rienstra, M. Auger, K.V. Lakshmi, R.G. Griffin, J. Chem. Phys. 103 (1995) 6951–6958.
[21] X. Zhao, W. Hoffbauer, J.S. Guenne, M.H. Levitt, Solid State NMR 26 (2004) 57–64.
[22] T.G. Oas, R.G. Griffin, M.H. Levitt, J. Chem. Phys. 89 (1998) 692–695.
[23] T. Gullion, J. Schaefer, J. Magn. Reson. 81 (1989) 196–200.
[24] Y.K. Lee, N.D. Kurur, M. Helmle, O.G. Johannessen, N.C. Nielsen, M.H. Levitt, Chem. Phys. Lett. 242 (1995) 304–309.
[25] M. Hohwy, H.J. Jacobsen, M. Eden, M.H. Levitt, N.C. Nielsen, J. Chem. Phys. 108 (1998) 2686–2694.
[26] M. Hohwy, C.M. Rienstra, C.P. Jaroniec, R.G. Griffin, J. Chem. Phys. 110 (1999) 7983–7992.
[27] A. Brinkmann, M. Eden, M.H. Levitt, J. Chem. Phys. 112 (2000) 8539–8554.
[28] M. Carravetta, M. Eden, X. Zhao, A. Brinkmann, M.H. Levitt, Chem. Phys. Lett. 321 (2000) 205–215.
[29] M. Veshtort, R.G. Griffin, J. Magn. Reson. 178 (2006) 248–282.
[30] M. Bak, N.C. Nielsen, J. Magn. Reson. 125 (1997) 132–139.
[31] M. Eden, M.H. Levitt, J. Magn. Reson. 132 (1998) 220–239.